Optical properties of Ag_29(BDT)_12(TPP)_4 in the VIS and UV and influence of ligand modeling based on real-time electron dynamics

Rajarshi Sinha-Roy, Xóchitl López-Lozano, Robert Whetten, H.C. Weissker

Noname manuscript No.
(will be inserted by the editor)

Optical Properties of $Ag_{29}(BDT)_{12}(TPP)_4$ in the VIS and UV and Influence of Ligand Modeling Based on Real-Time Electron Dynamics

Rajarshi Sinha-Roy · Xóchitl López-Lozano · Robert L. Whetten · Hans-Christian Weissker

Received: date / Accepted: date

Abstract We study the optical properties of the $Ag_{29}(BDT)_{12}(TPP)_4$ cluster, the geometry of which is available from experimental structure determination, by means of Fourier-transformed induced densities from real-time (time evolution) calculations of time-dependent density-functional theory. In particular, we demonstrate the influence of the ligands on the optical spectra in the visible region and, even more, in the UV. A strong peak in the UV reminiscent of the spectrum of isolated benzene is found to be caused by the phenyl rings of the TPP ligand molecules. Nonetheless, their absence in the modeling also impacts the absorption in the visible region substantially. By contrast, the aromatic rings of the BDT ligands are more strongly coupled to the silver core and loose the character of independent oscillators; they contribute a much less peaked UV absorption. Our results underline the importance of properly accounting for the full ligands for precise and reliable modeling.

Keywords Silver clusters · Optical response · Monolayer-protected clusters · Ligand modeling · TDDFT

Rajarshi Sinha-Roy, Laboratoire des Solides Irradiés, École Polytechnique, CNRS, CEA/DRF/IRAMIS, Institut Polytechnique de Paris, F-91128 Palaiseau, France *and* Aix-Marseille Univ., CNRS, CINAM, Marseille, France, *and* European Theoretical Spectroscopy Facility (www.etsf.eu) E-mail: rajarshi.sinha-roy@polytechnique.edu

Xóchitl López-Lozano, Department of Physics & Astronomy, The University of Texas at San Antonio, One UTSA circle, 78249-0697 San Antonio, TX., USA

Robert L. Whetten, Department of Applied Physics and Materials Science, and MIRA, Northern Arizona University, Flagstaff, Arizona 86011, USA

Hans-Christian Weissker, Aix-Marseille Univ., CNRS, CINAM, Marseille, France, *and* European Theoretical Spectroscopy Facility (www.etsf.eu) E-mail: weissker@cinam.univ-mrs.fr

1 Introduction:

The properties of noble-metal clusters are decisively different from those of the respective bulk metals owing to the confinement to very small sizes. Ranging from clusters of but a few atoms to nanoparticles of a few hundred nanometers in diameter, their study is of great importance for the understanding of fundamental questions concerning the physics of nanostructured metals. Wet-chemically produced monolayer-protected clusters play a particular role because many of them are stabilized in particular geometries which can be determined experimentally by x-ray crystallography. In recent years, total structure determination of a large number of monolayer-protected clusters has been accomplished [1,2], which provides the basis for the advanced study of their properties and, in particular, of structure-property relations.

The efforts of synthesis and total structure determination of monolayer-protected clusters were initially directed mostly at gold clusters due to the relatively high stability against oxidation and to their biocompatibility in view of applications like biomolecule labeling [3], inhibition of HIV fusion [4], or growth inhibition of bacteria [5].

However, silver clusters are likewise interesting for applications in view of their bactericidal effects [6–8]. They were likewise found to form ligand-protected "ultrastable" nanoparticles [9]. Recently, clusters of 29 silver atoms have been reported by different groups to show special stability and interesting optical properties [10–13]. A water-soluble variant, stabilized with lipoate (LA) ligands and tentatively identified as $Ag_{29}LA_{12}$ by analogy to the hydrophobic homologue $Ag_{29}(BDT)_{12}(TPP)_4$ determined by Abdul-Halim *et al.* [13] has been demonstrated to show antibacterial and antifungal activity [14].

In addition, doping of the silver clusters with gold atoms was shown to increase the stability of the clusters as well as their photoluminescence quantum yield [15]. Calculations of time-dependent density-functional theory (TDDFT) of these gold-doped clusters have been published by Juarez-Mosqueda *et al.* [16], focusing on the effect of the dopants and analyzing states and optical transitions. However, it appears that a detailed analysis of the pure $Ag_{29}(BDT)_{12}(TPP)_4$ has not been published.

Our present work focuses on the structure-determined form of Ref. [13], $Ag_{29}(BDT)_{12}(TPP)_4$ (BDT: 1,3-benzenedithiol; TPP: triphenylphosphine). In that publication, it is noted that the cluster in charge state -3 (three additional electrons) corresponds to a super-atom complex (SAC)[17] according to the electron counting rule, with an electron count of $n = 29 - 24 + 3 = 8$, thus corresponding to a shell filling $1S^2|1P^6$ and an expected large gap between the 1P and 1D SAC states. The article also contains a TDDFT calculation for which the phenyl rings of the TPP ligands were replaced by -H groups to save time, justified, according to the authors, by the fact that they are not involved in the frontier orbitals. However, no explicit test of the validity of this procedure for the calculation of the spectra was shown.

In the present work, we present a systematic study of the electronic structure and the optical response of $Ag_{29}(BDT)_{12}(TPP)_4$ using, in particular, the

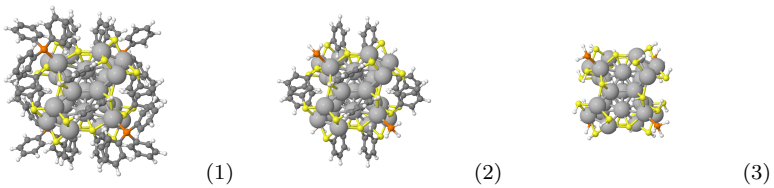

(1) (2) (3)

Fig. 1 Structure of the clusters used in the present work: (1) the full structure as taken from the original publication by the Bakr group [13]; (2) the same structure after replacement of the aromatic rings of the TPP ligands by hydrogen atoms as advocated in Ref. [13], and (3) a minimal model where all the ligands are replaced by hydrogen saturation.

analysis of the induced density from real-time TDDFT that some of the present authors tested and discussed recently [18]. In addition, we investigate the effect of the reduction of the ligands, comparing in detail the full structure, the structure with the phenyl rings of the TPP ligands cut off as used in Ref. [13], and a minimal model where all ligands are replaced by H saturation.

2 Models and Methods

We started from the experimentally determined coordinates of Ref. [13]. In addition to the full structure (1), we used two reduced models: (2) the structure with the phenyl rings of the TPP ligands cut off, reducing them to PH_3 (this is the model used in Ref. [13]), and (3) a minimal model where all the rings are replaced by hydrogens, i.e., $Ag_{29}(SH)_{24}(PH_3)_4$. The resulting structures are shown in Fig. 1. In all cases, the charge state -3 was used. The relaxation of the clusters was carried out using the `VASP` code [19,20] and the PW91 gradient-corrected functional [21].

The electronic states and the optical spectra have been calculated using DFT and TDDFT with the real-space code `octopus` [22–24]. Norm-conserving Troullier-Martins pseudopotentials have been used which include the d electrons in the valence, that is, with 11 valence electrons for each silver atom. The gradient-corrected PBE exchange-correlation potential has been used. The real-space grid spacing was set to 0.18 Å, the radius of the spheres around each atom that make up the calculation domain was set to 5 Å. The projected density of states was obtained from the ground state wave functions of the `octopus` calculation using the recipe as detailed in ref. [17]. Details are described in the Supplementary Information.

Optical spectra were calculated using the Yabana-Bertsch time-evolution formalism [25] of TDDFT. The ETRS propagator ("enforced time-reversal symmetry") was used. Propagation time was 25 fs.

In order to analyze the electronic modes contributing to the individual features in the absorption spectra, we used the Fourier-transform analysis of the time-dependent induced density that some of the present authors recently presented and analyzed in detail [18]. The method is briefly described in the Supplementary Information. The time-dependent induced densities for each

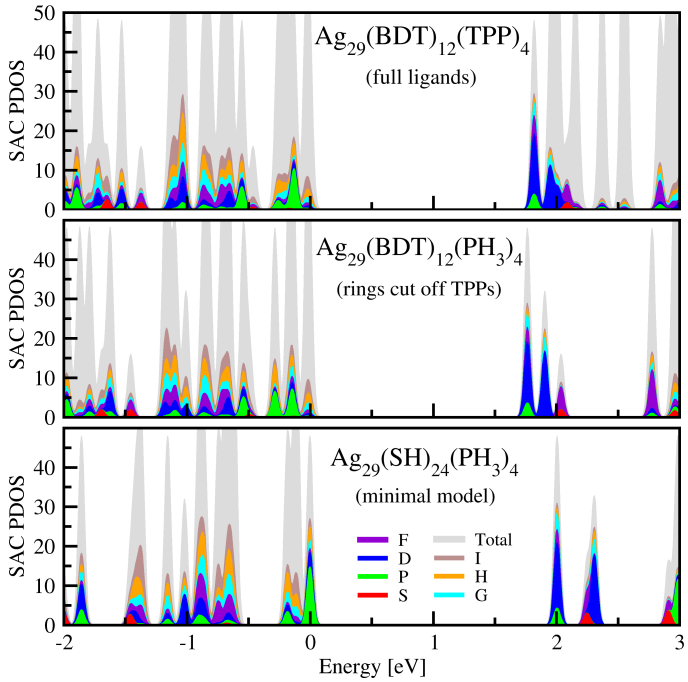

Fig. 2 SAC projected density of states of the experimental structure (1) with the complete ligands and of the two reduced models. The zero of the energy axis is the HOMO energy in all cases.

25th time-step were used to perform the Fourier transformation at each of the grid points. The grid spacing (0.18 Å), the interval between two consecutive time-steps (dt=0.0024$\hbar$/eV), and the total time of evolution (15625*dt) were chosen to be the same as in the `octopus` simulation for the corresponding spectra. A damping of 0.0037 atomic unit of energy (0.1 eV) was chosen for the exponential window function during the Fourier transform. The modes of induced density corresponding to optical absorption at a given energy are shown as the Fourier sine coefficients which were written out for 500 equally spaced frequency points between 0 and 0.3 atomic units of energy (8.1 eV). Graphics of induced densities were prepared with the UCSF Chimera package [26].

3 Results and Discussion:

To study and quantify the differences incurred by the simplifications of the full ligands, we have analyzed the inter-atomic distances between the silver atoms in the three relaxed structures. Most of the Ag-Ag bonds do not change strongly upon removal of the phenyl rings from the TPP ligands, as can be seen in Supplementary Figure S1. However, those which are the most directly connected to the P atoms, viz., the sides of the triangular pyramids pointing outward to the silver atoms to which the P atoms are bound, shorten very

strongly, from 3.55 to 3.18 Å(labeled g in Supplementary Figure S1). A similar effect is seen on the 12 bonds pointing outward on the rectangular triangular "towers" labeled f, which shorten strongly upon removal of the BDT ligands in structure (3).

The electronic structure of the cluster and of the two simplified models is shown in Fig. 2, the energies of the states around the HOMO-LUMO gap in Supplementary Figure S2. The individual states are shown in the Supplementary Figures S3, S4, and S5. We confirm the designation of the cluster as a 8-electron superatom complex. However, in our calculations of the full structure, the three SAC 1P states lie 0.13 eV *below* a group of non-SAC states that constitute the HOMO. The LUMO, by contrast, corresponds indeed to the five 1D states.

This situation is not very different in structure (2) after removal of the TPP ligands' phenyl rings, except that one more state approaches the energy of the (non-SAC) HOMO group of states. Finally, the removal of all the rings in the minimal model (3) turns out to represent the essence of the SAC structure: here, the frontier orbitals are indeed the SAC P and D states. Fig. 2 shows that their energy difference remains roughly unchanged between the three structures; it is the fact that other states enter between them and constitute the HOMO in the first two cases that the gap is slightly smaller for them compared to the minimal model.

The absorption spectra are shown in Fig. 3. The VIS spectrum of the full structure is characterized by a shoulder at 2.20 eV and three peaks at 2.68, 2.95, and 3.27 eV. In addition, a very strong peak in the UV, at 6.68 eV is visible. We note that our result agrees with the spectrum of the pure silver cluster included in Ref. [16].

The spectrum of structure (2) (rings cut off from the TPP ligands) retains a certain similarity to that of the complete structure (1), but the differences even in the lower VIS portion of the spectrum are very strong. In particular, the intensities of the different peaks are very different. We conclude that the replacement of the rings on the TPP ligands is not an option for the reliable calculation of the spectra in the VIS, in spite of the fact that they do not contribute to the frontier orbitals [13]. In addition, the strong peak at 6.68 eV has almost completely vanished, pointing to the fact that it originates to a large part from the phenyl rings, as will be discussed below.

For the minimal model, structure (3), the resemblance in the VIS is essentially lost, the spectra are very different and more peaked (doubtless due to the lower number of transitions available). The high-energy peak in the UV is entirely missing and replaced by a background of unspecific absorption.

All these findings point to the importance of the ligands for the optical properties. We will now analyze the respective transitions using our tool of

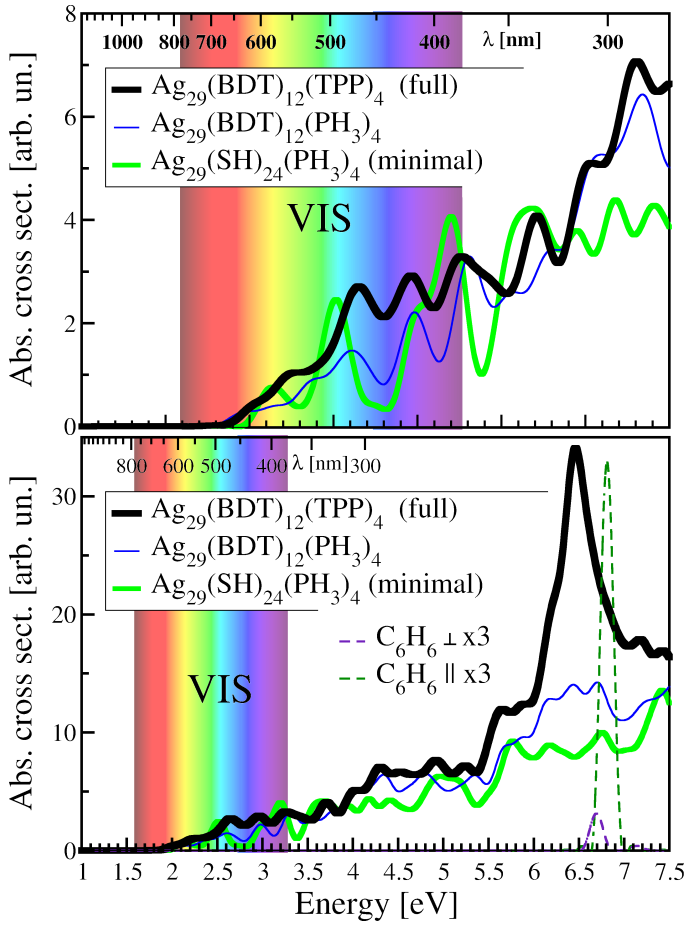

Fig. 3 Spectra of monolayer-protected Ag_{29} calculated for the three structures using real-time TDDFT showing the VIS part of the spectrum (upper panel) and a wider range including the high-energy peak at 6.5 eV (lower panel). In all cases, the charge state of -3 was used. In addition, the spectra of benzene are added in the lower panel for excitation perpendicular and parallel to the ring.

spatially resolved Fourier transform on the induced density from a real-time ("time evolution) TDDFT calculation [18].

In Fig. 4 we show the Fourier-transformed induced densities of the full cluster at 3 energies in the VIS, 2.68, 2.95, and 3.27 eV. They show that these three peaks are mainly due to contributions in the silver "core," although coupled to contributions in the ligands. This includes small but real contributions from the four TPP ligands, which in turn explains well the differences between the spectra of the full structure (1) and the structure (2) where the TPP ligands have been reduced to PH_3. The contributions in the BDT ligands are stronger, which in turn explains the complete change of the spectra if these are removed, as in the minimal model structure (3). The low-energy shoulder

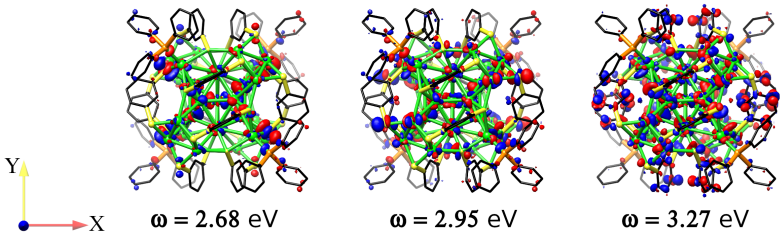

Fig. 4 Fourier-transformed induced densities in $Ag_{29}(BDT)_{12}(TPP)_4$ at energies (in the VIS) of 2.68, 2.95, and 3.27 eV are shown for an iso-surface value of $\pm 2 \times 10^{-7}$ (red and blue), along with the atomic arrangements in the cluster. The perturbation was applied along the x axis. We show the reconstructed modes at a quarter period, details are explained in the Supplementary Material.

at 2.20 eV (not shown) is clearly due to an excitation in the silver core, with negligible contribution from the ligands.

The high-energy UV peak at 6.68 eV is caused principally by the excitation of the ligand rings, which is clearly visible in the isosurface representation of the induced densities in the left panel of Fig. 5. This is also clearly corroborated by the similarity of the high-energy peak to the spectra of pure, isolated benzene as shown in the lower panel of Fig. 3. The isosurface representation in Fig. 5 shows clearly that *all the rings contribute,* those of the TPP *and* those

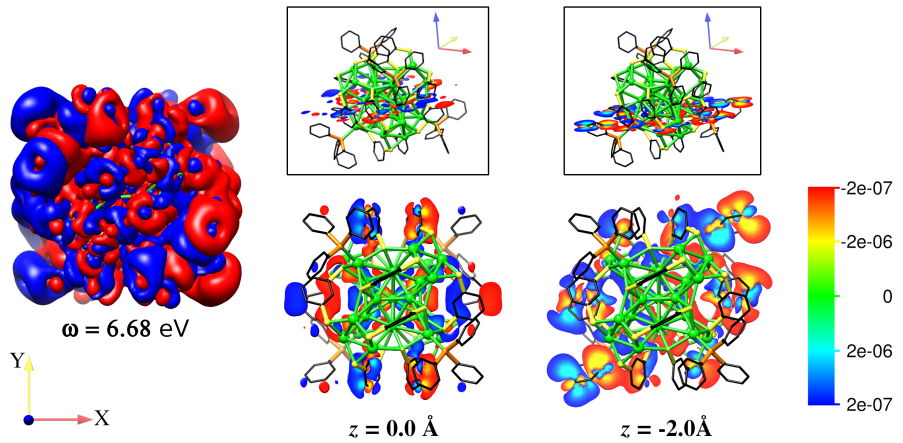

Fig. 5 Fourier-transformed induced density corresponding to the high-energy UV peak at 6.68 eV in $Ag_{29}(BDT)_{12}(TPP)_4$ is shown (at left) as an iso-surface with $\pm 2 \times 10^{-7}$ iso-value, and as surface color maps for two different slabs in the x-y plane, at $z = 0.0$ Å (through the center of the cluster) and $z = -2.0$ Å; the position of the slabs are indicated in the framed insets. The slab through the center (at $z = 0.0$) of the cluster does not cut through the rings of the TPP ligands but shows the contribution of the BDT rings. By contrast, the value of $z = 2.0\,\AA$ for the second slab has been chosen to highlight the contribution in the TPP rings. The perturbation is applied along the x axis. Values for different color are shown in the color bar.

of the BDT ligands. However, there is clearly a difference, as suggested by the difference in the spectra: after removal of the phenyl rings of the TPP ligands, the high-energy peak of the full cluster (1) is strongly reduced and replaced by a bump in the spectra consisting of a number of low-intensity peaks. The difference between this spectrum of structure (2) and that of the minimal model (3) are due to the contributions of the BDT rings, clearly broadened and deviating from the excitations of the isolated benzene due to strong coupling to the silver "core" of the cluster. Also, the contributions from the aromatic rings of the BDT ligands are weaker than those of the TPP phenyl rings. This can be clearly seen in the color map representation of the slabs in Fig. 5, where the relative values of the induced density around the BDT ligands are much smaller than the values around the phenyl rings of the TPP ligands. We infer from this that the coupling of the BDT rings via the S atoms makes them lose their quality as independent resonators. Indeed, the spectrum between 6 and 7 eV is not strikingly different from that of the minimal structure (3) in which all the aromatic ligand rings have been removed.

4 Conclusions

We have carried out an analysis of the optical spectra of $Ag_{29}(BDT)_{12}(TPP)_4^{-3}$ in view of the nature of the excitations and of the influence of the different ligands present in the structure. The customary procedure of truncating the TPP ligands, justified by the assumption that they are not involved in the frontier orbitals, gives a decent description of the states around the HOMO-LUMO gap, but it easily leads to questionable results for the optical spectra in the visible region (and beyond, of course.) We find that the truncation changes some of the silver bonds of the outer part of the silver core strongly, which leads to modifications in the order of the electronic states. The cluster is indeed a 8-atom super-atom complex, but in our calculations, 5 states mostly localized in the ligands are found inside the SAC gap; the HOMO group of states does not consist of SAC states.

We analyzed the excitations that appear in the absorption spectra using spatially resolved Fourier-transform of the induced densities of the time-evolution TDDFT calculation. The spectra in the VIS are due to excitations mostly localized in the core but coupled to contributions from the ligands. This coupling is sufficient to render the above-mentioned truncation of the TPP rings inadequate for the description of the spectra in the VIS region. The high-energy UV peak is mainly due to the TPP ligands, their phenyl rings constituting almost independent oscillators. It is strongly diminished when the rings are cut-off. By contrast, the aromatic rings of the BDT ligands are much more strongly coupled to the excitations of the core; their absence changes the spectra entirely even in the visible region. Our analysis shows that, for the reliable calculation of even the visible region, the full structure including all parts of the ligands needs to be treated.

5 Acknowledgments

We thank Pablo García González for enlightening discussions. This work has been carried out in part thanks to the support of the A*MIDEX grant (n°ANR-11-IDEX-0001-02) funded by the French Government "Investissements d'Avenir" program. We acknowledge support from the French National Research Agency (Agence Nationale de Recherche, ANR) in the frame of the project "FIT SPRINGS", ANR-14-CE08-0009. This work has used HPC resources from GENCI-IDRIS (Grant 2018-096829). Moreover, HCW and RSR would like to acknowledge the contribution of the International Research Network IRN Nanoalloys (CNRS).

References

1. Y. Negishi, T. Nakazaki, S. Malola, S. Takano, Y. Niihori, W. Kurashige, S. Yamazoe, T. Tsukuda, H. Häkkinen, Journal of the American Chemical Society **137**(3), 1206 (2015). DOI 10.1021/ja5109968. URL http://dx.doi.org/10.1021/ja5109968. PMID: 25549276
2. R. Jin, Y. Pei, T. Tsukuda, Accounts of Chemical Research **52**(1), 1 (2019). DOI 10.1021/acs.accounts.8b00631
3. C.J. Ackerson, R.D. Powell, J.F. Hainfeld, in *Cryo-EM Part A Sample Preparation and Data Collection*, *Methods in Enzymology*, vol. 481, ed. by G.J. Jensen (Academic Press, 2010), pp. 195 – 230. DOI http://dx.doi.org/10.1016/S0076-6879(10)81009-2. URL http://www.sciencedirect.com/science/article/pii/S0076687910810092
4. M.C. Bowman, T.E. Ballard, C.J. Ackerson, D.L. Feldheim, D.M. Margolis, C. Melander, Journal of the American Chemical Society **130**(22), 6896 (2008). DOI 10.1021/ja710321g. URL http://pubs.acs.org/doi/abs/10.1021/ja710321g
5. J. Bresee, K.E. Maier, A.E. Boncella, C. Melander, D.L. Feldheim, Small **7**(14), 2027 (2011). DOI 10.1002/smll.201100420. URL http://dx.doi.org/10.1002/smll.201100420
6. M. Rai, A. Yadav, A. Gade, Biotechnology Advances **27**(1), 76 (2009)
7. N.V. Ayala-Núñez, H.H. Lara Villegas, L. del Carmen Ixtepan Turrent, C. Rodríguez Padilla, NanoBiotechnology **5**(1), 2 (2009)
8. H.H. Lara, E.N. Garza-Treviño, L. Ixtepan-Turrent, D.K. Singh, Journal of Nanobiotechnology **9**(1), 30 (2011)
9. A. Desireddy, B.E. Conn, J. Guo, B. Yoon, R.N. Barnett, B.M. Monahan, K. Kirschbaum, W.P. Griffith, R.L. Whetten, U. Landman, T.P. Bigioni, Nature **501**, 399 (2013). DOI 10.1038/nature12523
10. J. Kumar, T. Kawai, T. Nakashima, Chem. Commun. **53**, 1269 (2017)
11. M. van der Linden, A. Barendregt, A.J. van Bunningen, P.T.K. Chin, D. Thies-Weesie, F.M.F. de Groot, A. Meijerink, Nanoscale **8**, 19901 (2016)
12. I. Russier-Antoine, F. Bertorelle, R. Hamouda, D. Rayane, P. Dugourd, Z. Sanader, V. Bonacic-Koutecky, P.F. Brevet, R. Antoine, Nanoscale **8**, 2892 (2016)
13. L.G. AbdulHalim, M.S. Bootharaju, Q. Tang, S. Del Gobbo, R.G. AbdulHalim, M. Eddaoudi, D.e. Jiang, O.M. Bakr, Journal of the American Chemical Society **137**(37), 11970 (2015). DOI 10.1021/jacs.5b04547
14. P. Lopez, H.H. Lara, S. M. Mullins, D. M. Black, H. M. Ramsower, M.M. Alvarez, T.L. Williams, X. Lopez-Lozano, H.C. Weissker, A.P. GarcÃa, I.L. Garzón, B. Demeler, J.L. Lopez-Ribot, M.J. YacamÃ¡n, R.L. Whetten, ACS Applied Nano Materials **1**(4), 1595 (2018). DOI 10.1021/acsanm.8b00069
15. G. Soldan, M.A. Aljuhani, M.S. Bootharaju, L.G. AbdulHalim, M.R. Parida, A.H. Emwas, O.F. Mohammed, O.M. Bakr, Angewandte Chemie International Edition **55**(19), 5749 (2016)

16. R. Juarez-Mosqueda, S. Malola, H. Hakkinen, Phys. Chem. Chem. Phys. **19**, 13868 (2017). DOI 10.1039/C7CP01440F
17. M. Walter, J. Akola, O. Lopez-Acevedo, P.D. Jadzinsky, G. Calero, C.J. Ackerson, R.L. Whetten, H. Grönbeck, H. Häkkinen, Proceedings of the National Academy of Sciences **105**(27), 9157 (2008). DOI 10.1073/pnas.0801001105. URL http://www.pnas.org/content/105/27/9157.abstract
18. R. Sinha-Roy, P. García-González, X. López Lozano, R.L. Whetten, H.C. Weissker, Journal of Chemical Theory and Computation **14**, 6417 (2018). DOI 10.1021/acs.jctc.8b00750
19. G. Kresse, J. Furthmüller, Comput. Mat. Sci. **6**, 15 (1996)
20. G. Kresse, D. Joubert, Phys. Rev. B **59**, 1758 (1999)
21. J.P. Perdew, Y. Wang, Phys. Rev. B **45**, 13244 (1992)
22. M.A.L. Marques, A. Castro, G.F. Bertsch, A. Rubio, Comp. Phys. Comm. **151**, 60 (2003)
23. A. Castro, M.A.L. Marques, H. Appel, M. Oliveira, C. Rozzi, X. Andrade, F. Lorenzen, E.K.U. Gross, A. Rubio, Phys. Stat. Sol. (b) **243**, 2465 (2006)
24. N. Tancogne-Dejean, M.J.T. Oliveira, X. Andrade, H. Appel, C.H. Borca, G. Le Breton, F. Buchholz, A. Castro, S. Corni, A.A. Correa, U. De Giovannini, A. Delgado, F.G. Eich, J. Flick, G. Gil, A. Gomez, N. Helbig, H. HÃ¼bener, R. Jestädt, J. Jornet-Somoza, A.H. Larsen, I.V. Lebedeva, M. Lüders, M.A.L. Marques, S.T. Ohlmann, S. Pipolo, M. Rampp, C.A. Rozzi, D.A. Strubbe, S.A. Sato, C. Schäfer, I. Theophilou, A. Welden, A. Rubio, The Journal of Chemical Physics **152**(12), 124119 (2020)
25. K. Yabana, G.F. Bertsch, Phys. Rev. B **54**, 4484 (1996). DOI 10.1103/PhysRevB.54.4484. URL http://link.aps.org/doi/10.1103/PhysRevB.54.4484
26. E.F. Pettersen, T.D. Goddard, C.C. Huang, G.S. Couch, D.M. Greenblatt, E.C. Meng, T.E. Ferrin, Journal of Computational Chemistry **25**(13), 1605 (2004). DOI 10.1002/jcc.20084. URL https://onlinelibrary.wiley.com/doi/abs/10.1002/jcc.20084